A Letters Journal Exploring the Frontiers of Physics

August 2018

EPL, **123** (2018) 48003 www.epljournal.org
doi: 10.1209/0295-5075/123/48003

Nonstationary chimeras in a neuronal network

Zhouchao Wei[1], Fatemeh Parastesh[2], Hamed Azarnoush[2], Sajad Jafari[2], Dibakar Ghosh[3], Matjaž Perc[4,5,6(a)] and Mitja Slavinec[4]

[1] *School of Mathematics and Physics, China University of Geosciences - Wuhan, 430074, China*
[2] *Department of Biomedical Engineering, Amirkabir University of Technology - 424 Hafez Ave., Tehran 15875-4413, Iran*
[3] *Physics and Applied Mathematics Unit, Indian Statistical Institute - 203 B. T. Road, Kolkata 700108, India*
[4] *Faculty of Natural Sciences and Mathematics, University of Maribor - Koroška cesta 160, SI-2000 Maribor, Slovenia*
[5] *Complexity Science Hub - Josefstädterstraße 39, A-1080 Vienna, Austria*
[6] *School of Electronic and Information Engineering, Beihang University - Beijing 100191, China*

received 29 June 2018; accepted in final form 20 August 2018
published online 18 September 2018

PACS 89.75.-k – Complex systems
PACS 05.45.Xt – Synchronization; coupled oscillators

Abstract – Chimeras are special states that are composed of coexisting spatial domains of coherent and incoherent dynamics, which typically emerge in identically coupled oscillators. In this paper, we study a network of nonlocally coupled Hindmarsh-Rose neurons that are subject to an alternating current. We show that chimera states emerge when the neurons are connected through electrical synapses. The considered model has two coexisting attractors, namely a limit cycle and a chaotic attractor, to which the dynamics converges in dependence on the initial conditions. While earlier research reported the existence of chimeras in Hindmarsh-Rose neuronal networks mainly through chemical synapses, here we show that an alternating current in an electrically coupled network can also evoke chimeras, whereby the spatial positions of coherent and incoherent domains vary with time. Remarkably, we also observe chimera states in locally coupled neurons through electrical synapses, which reduce the relaxation of nonlocallity in the coupling configuration. The existence of nonstationary chimeras is confirmed by means of a local order parameter.

Introduction. – Different oscillatory networks exist in nature, which typically evolved either completely synchronous or asynchronous states. Chimeras, or chimera states, are in this regard special because they are characterized by the coexistence of spatial organized subpopulations of coherent and incoherent dynamics [1–3]. Chimeras have received ample attention [4–7] in various fields after their discovery in nonlocally coupled phase oscillators in 2002 [8]. Apart from the fascinating nature in theoretical studies, chimeras have also found to be related to different real-life phenomena, including unihemispheric sleep in birds and dolphins [9], epileptic seizures [10], modular neural networks [11], and even to some aspects of social systems [12].

The chimera states were firstly observed in a network of nonlocally coupled complex Ginzburg-Landau phase oscillators [8]. Chimeras have also been investigated with either global, local or nonlocal coupling [13–15], in periodic oscillators [16], chaotic oscillators and maps [17,18], and also in different neuronal systems [19–22]. In 2013, Hizanidis *et al.* [20] studied the occurrence of chimera states for various coupling schemes in networks of two- and three-dimensional Hindmarsh-Rose oscillators. Bera *et al.* [19] investigated the existence of chimera states in pulse-coupled networks of bursting Hindmarsh-Rose neurons using a chemical synaptic coupling function. Majhi *et al.* [21] considered a network of neurons with multilayer structure and examined the impact of homogeneous and heterogeneous information transmission delays on the chimera states. Recently, Shepelev *et al.* [22] discovered new chimera patterns in a ring of nonlocally coupled FitzHugh-Nagumo oscillators. Besides these, chimera states have been verified experimentally in different oscillator types such as chemical [23], optical [24], and

(a) E-mail: matjaz.perc@uni-mb.si

mechanical systems [25]. Depending on the different spatiotemporal patterns, many new types of chimera states have been identified including amplitude chimeras [26], chimera death [27,28], breathing chimeras [29], imperfect chimeras [30,31], traveling chimeras [32], alternating chimera [33] and even spiral wave chimeras [34].

Here we consider the dynamics in a ring network, where the local dynamics of each node is described by the modified Hindmarsh-Rose (HR) neuron model [35–37]. In neuronal networks, the neurons are connected by two different synapses, namely the electrical and chemical synapses [19–21,38,39]. If the synaptic coupling is chemical, a nonlinear sigmoidal function with a threshold and saturation constants are used to define it. For electrical synaptic coupling, a linear function which depends on the difference between the membrane potentials is used. More precisely, we here consider a network of nonlocally coupled alternating-current–induced Hindmarsh-Rose neurons [37]. This model is interesting due to the bistability nature, *i.e.*, a stable periodic limit cycle coexists with a chaotic attractor. Which is ultimately selected by the trajectory depends on the initial conditions. This setup thus promises fascinating spatiotemporal dynamics, as we will demonstrate in what follows. In most of the previous works [19–21] on chimera states in neuronal networks, the observed chimeras are stationary in patterns. But in some neuronal processes, such as in bump states, the spatial positions of neurons in coherent and incoherent states are not static with respect to time. Thus, the systematic study on nonstationary chimera states in neuronal networks deserves special attention.

In this letter, we study the emergence of nonstationary chimera states in nonlocally coupled neuronal networks. We consider the local dynamics of each node by a HR neuronal model with alternating current on the membrane potential which makes the system bistable. The presence of alternating current in the individual node plays a crucial role for the emergence of nonstationary chimera states. We identify and confirm the new nonstationary chimera states using the local order parameter. The earlier studies on chimera states in neuronal networks, it was observed that the obtained chimeras were stationary, *i.e.*, the coexistence of coherent and incoherent groups in chimera state are not changed with respect to time. Remarkably, we find that the chimera state also emerges in locally coupled neurons through electrical synapses whereas previous work [20] demanded that a nonlocal coupling configuration with rectangular kernel is necessary for the existence of chimera states in electrically coupled neurons. We further identify the transition of incoherent, chimera and coherent states by varying the coupling strength and the number of nearest neighbors in the nonlocal ring. The obtained chimera states are confirmed by the calculation of the local order parameter.

Mathematical form of neuronal network model. – The Hindmarsh-Rose neuron model is used extensively to describe dynamical patterns of the membrane potential. Here as a single unit of the network, we consider an improved version of the HR neuron model proposed by Bao *et al.* [37] with an injected external alternating current on the membrane potential in the axon of a neuron. The mathematical form of the modified HR neuronal model is described as

$$\begin{aligned} \dot{x} &= y + 3x^2 - x^3 - z + 3 + I_m \sin(2\pi F t), \\ \dot{y} &= 1 - 5x^2 - y, \\ \dot{z} &= 0.0084(x + 1.6) - 0.0021z, \end{aligned} \tag{1}$$

where x represents the membrane potential in the axon of a neuron, y and z are the spiking and bursting variables which are used to exchange fast (associated with Na^+ or K^+) and slow (associated with Ca^{2+}) currents, respectively. Here I_m and F are, respectively, the amplitude and frequency of the injected external alternating current. In this modified HR model, alternating current induces different coexisting behaviors of asymmetric bursters for different parameter values of I_m and F. For fixed values of $I_m = 1.2$ and $F = 0.05$, the modified HR neuronal model exhibits two coexistence states. For the initial conditions $(0, 0, 0)$ and $(0, 0, 6)$, a stable limit cycle and a chaotic attractor emerge and the phase-space diagrams are shown in fig. 1(a). These two coexisting states are also confirmed by the calculation of the Lyapunov exponent. The variations of the maximum Lyapunov exponent (MLE) for limit cycle and chaotic attractor are shown in fig. 1(b) by blue and gray lines, respectively. To explore the complete scenario of the coexisting states (limit cycle and chaotic), we compute the basin of attraction of the model (1) by changing the initial conditions $x_0 = y_0$ and z_0. The basin of attraction for the isolated neuronal HR model is shown in fig. 2. The blue and gray regions correspond to the initial conditions for stable limit cycle and chaotic attractor states, respectively. From this figure, it is noticed that the initial conditions of the bursting variable z is vital for the

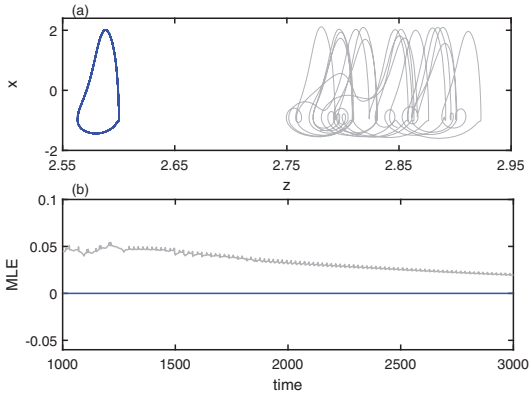

Fig. 1: (Colour online) (a) A limit cycle coexists with a chaotic attractor at $I_m = 1.2$ and $F = 0.05$ with initial conditions respectively at $(0, 0, 0)$ (blue) and $(0, 0, 6)$ (gray). (b) Variation of the maximum Lyapunov exponent (MLE) to confirm periodic and chaotic behaviors.

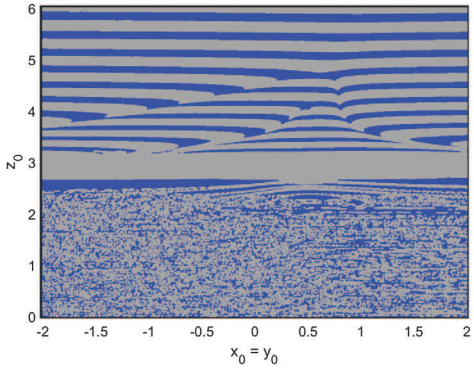

Fig. 2: (Colour online) Basin of attraction of the isolated HR neuronal model (1) for $I_m = 1.2$ and $F = 0.05$. Blue and gray regions represent the initial conditions for limit cycle and chaotic attractor, respectively.

emergence of coexisting states. For $z_0 \leq 2.4$, the initial conditions for limit cycle and chaotic state are intertwined and after that value there is a well-separated basin of attractions for limit cycle and chaotic states.

Next, we consider a network of nonlocally coupled alternating-current–induced HR neurons which are conected with each other through electrical synapses. The mathematical form of the coupled network is written as

$$\begin{aligned} \dot{x_i} &= y_i + 3x_i^2 - x_i^3 - z_i + 3 + 1.2\sin(0.1\pi t) \\ &\quad + \frac{d}{2P}\sum_{j=i-P}^{i+P}(x_j - x_i), \\ \dot{y_i} &= 1 - 5x_i^2 - y_i, \\ \dot{z_i} &= 0.0084(x_i + 1.6) - 0.0021 z_i,\ i = 1, 2, \ldots, N, \end{aligned} \tag{2}$$

where d represents the coupling strength which determines how the information is exchanged among the neurons through electric synapses, each neuron in the network is coupled to its P number of nearest neighbors on both sides. Next our main target is to investigate the different spatiotemporal dynamics by changing the parameters d and P. In the numerical simulations, we choose $N = 100$ number of neurons and use the fourth-order Runge-Kutta method with time step 0.01.

Results. – We fix the number of nearest neighbor at $P = 20$ and vary the synaptic coupling strength d. We set the initial conditions as follows: $x_0(i) = y_0(i) = a_1(\frac{N}{2} - i)$ and $z_0(i) = 2.75 + a_2(N + 1 - i)$, where $a_1 = 0.04, a_2 = 0.002$. With these values of a_1 and a_2, the initial conditions lie between $x_0 = y_0 \in [-2, 2]$ and $z_0 \in [2.75, 2.95]$ for which each isolated neuron exhibits a chaotic state (cf. fig. 2). For smaller values of d, the neurons are in the incoherent state. The snapshots of the neurons at $d = 0.1$ are shown in fig. 3(a). With increasing value of $d = 0.65$, we observe that coupled neurons enter into a state with coexistence of synchronized and desynchronized neurons, which is a signature of the chimera state. The snapshot of the neurons at chimera state is depicted in fig. 3(b). With higher values of the synaptic coupling strength $d = 2.5$,

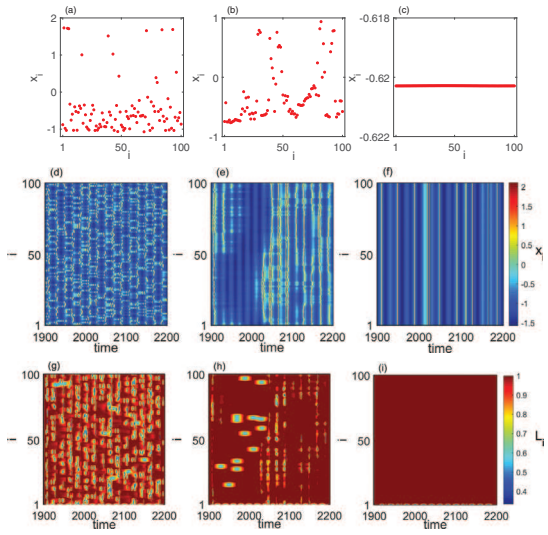

Fig. 3: (Colour online) The snapshot of the neurons at $t = 2050$ shows (a) the incoherent state at $d = 0.1$, (b) the chimera state at $d = 0.65$ and (c) the coherent state at $d = 2.5$. The second row shows the long-term behavior of the neurons corresponding to the first row, *i.e.*, (d) incoherent, (e) chimera, and (c) coherent state. Spatiotemporal patterns of the local order parameters for each neuron corresponding to the states in the second row. The initial conditions are selected where each isolated neuron is in the chaotic state.

all the neurons are in the synchronized state (fig. 3(c)). The long-term evolutions of the neurons for the incoherent, chimera and coherent states are respectively shown in figs. 3(d)–(f). From fig. 3(e), the spatiotemporal plot of the neurons in the chimera state, it is noticed that the synchronized and desynchronized domains in the chimera state are not static but travel with time. This is a clear signature of the nonstationary chimera state. Previously, nonstationary two-cluster chimera states were observed in a nonlocally coupled complex Ginzburg-Landau oscillator in the limit of strong coupling [40]. Bera *et al.* [41] investigated imperfect travelling chimera states in the HR neuronal model where a chemical synaptic coupling function was used. Recently, Majhi *et al.* [33] observed an alternating chimera state in an ephaptically coupled bursting HR neuronal network.

To quantify the spatial coherence-incoherence pattern and chimera state, we calculate the real-valued local order parameter [41] of each neuron. Note that the observed chimera state is nonstationary, so the strength of incoherence and mean phase velocity are not suitable measurements. The local order parameter is basically the local ordering of the neurons in coherent and incoherent groups. The local order parameter is defined as

$$L_i = \left| \frac{1}{2\delta} \sum_{|i-k| \leq \delta} e^{j\phi_k} \right|, \qquad i = 1, 2, \cdots, N \tag{3}$$

where δ is the number of nearest neurons on both sides of the i-th neuron. The geometric phase of the k-th neuron

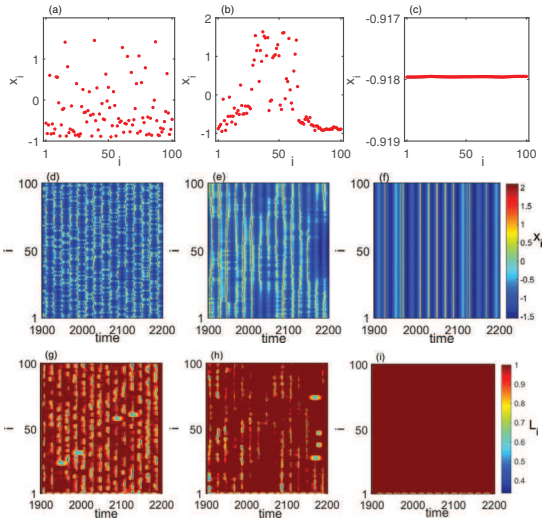

Fig. 4: (Colour online) The snapshots show the (a) incoherent state at $d = 0.25$, (b) the chimera state at $d = 0.67$ and (c) the coherent state at $d = 2.8$ at time $t = 2148$. The second and third rows indicate the spatiotemporal plots by taking long-time iteration of membrane potential and local order parameter, respectively.

is determined by the formula

$$\phi_k(t) = \frac{2\pi(t - t_i(n))}{t_i(n+1) - t_i(n)}, \tag{4}$$

where $t_i(n)$ is the time at which the n-th peak of the i-th neuron occurs and $t_i(n) \leq t \leq t_i(n+1)$. In order to calculate the local order parameter L_i, we use the spatial-window size $\delta = 1$ elements. When the local order parameter L_k is equal to 1, it indicates that the k-th neuron belongs to the coherent part of the chimera state, and when it is less than 1, it belongs to incoherent parts. Figures 3(g)–(i) show the variation of the local order parameter of each neuron for a long time of interval where the gray portion represents the coherent neurons in the chimera state.

Similarly, we also observe the nonstationary chimera state for the other choice of initial conditions. We set the initial conditions as $x_0(i) = y_0(i) = b_1(\frac{N}{2} - i)$ and $z_0(i) = b_2(N + 1 - i)$, where $b_1 = 0.04$, and $b_2 = 0.02$. With these values of b_1 and b_2, the initial conditions lie in the intertwining part where the basin of attraction for limit cycle and chaotic attractor are not well separated (cf. fig. 2). The first, second and third rows of fig. 4 respectively display the snapshot, spatiotemporal plots of membrane potential and local order parameter for incoherent (at $d = 0.25$), chimera (at $d = 0.67$) and coherent (at $d = 2.8$) states. Here the observed chimera state is also nonstationary. This nonstationary behavior in the chimera state emerges due to the presence of alternating current in the HR neuronal model, eq. (1).

Next we check the complete scenario of incoherent, chimera and coherent states by simultaneously varying the number of nearest-neighbor nodes P in the nonlocal coupling and synaptic coupling strength d. We vary P from 1 to 50 (*i.e.*, from local to global coupling configurations) and d from 0 to 3. Figure 5 shows the (d, P) two-parameter phase diagram for incoherent, chimera and coherent states. To plot this phase diagram we use the initial conditions as $x_0(i) = y_0(i) = c_1(\frac{N}{2} - i)$ and $z_0(i) = c_2(N + 1 - i)$, where $c_1 = 0.04$ and $c_2 = 0.06$. Remarkably, we note that the nonstationary chimera state is also observed in locally and globally coupled neurons through electric synaptic coupling. For an exemplary value, $P = 1$ and $d = 1.5$, we observe the chimera state in locally coupled neurons. Previously, the chimera state was also noticed in locally coupled oscillators due to the nonlinearity present in the coupling function [42]. The spatiotemporal plot and snapshot of the neurons in locally coupled neuron through electrical synaptic coupling are shown in figs. 6 (a) and (b), respectively.

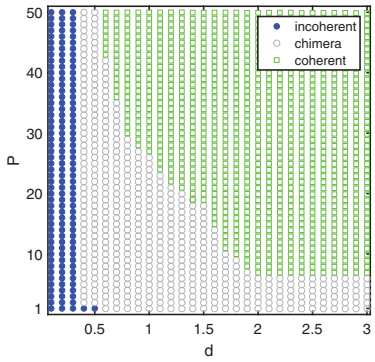

Fig. 5: (Colour online) The two-parameters phase diagram in the d-P plane depicts incoherent (blue filled circle), chimera (gray open circle) and coherent (green square) states.

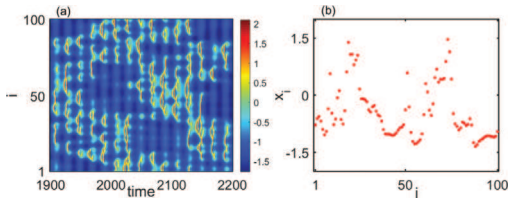

Fig. 6: (Colour online) Chimera state using locally connected neurons: (a) spatiotemporal pattern and (b) snapshot at $t = 2150$ of the network. Here $p = 1$ and $d = 1.5$.

Conclusions. – We have studied the dynamics of a neuronal network on the top of a ring topology, consisting of coupled Hindmarsh-Rose neurons with an alternating-current induction through electrical synapses. Actually, we have used an updated Hindmarsh-Rose model, which is characterized by bistability. In particular, the model exhibits the coexistence of periodic and chaotic attractor, as shown in fig. 1 and corresponding basin of attraction in fig. 2. To confirm different dynamical states, we have calculated the local order parameter for different values of the coupling strength d and number of nearest neighbors P in nonlocal coupling. We have shown that, in contrast

to a similar research done in the recent past, in our case the coupled system produces the chimera state which is not static, *i.e.*, the position of coherent and incoherent groups in the chimera state varies with time. We note that, typically, chimeras also occur in a locally coupled neuronal network where the coupling function is simple diffusive, *i.e.*, through electrical synapses.

More interestingly, we checked that nonstationary chimeras in our system can be observed even if the coupling configuration is all-to-all (global) (results are not shown here). The presented results could be of relevance for neuronal evolution, where the coexistence of coherent and incoherent dynamics during the developmental stage is likely to play an important role in the formative processes of the brain.

* * *

This work was supported by the Natural Science Foundation of China (Grant 11772306), by the Scientific Research Program of Hubei Provincial Department of Education (Grant B2017599), by the Department of Science and Technology, Government of India (Grant EMR/2016/001039), and by the Slovenian Research Agency (Grants J1-7009 and P5-0027). We also gratefully acknowledge S. Kundu, S. Majhi, and B. K. Bera for their insightful advice and discussions.

REFERENCES

[1] Jaros P., Borkowski L., Witkowski B., Czolczynski K. and Kapitaniak T., *Eur. Phys. J. ST*, **224** (2015) 1605.
[2] Jaros P., Maistrenko Y. and Kapitaniak T., *Phys. Rev. E*, **91** (2015) 022907.
[3] Maistrenko Y., Brezetsky S., Jaros P., Levchenko R. and Kapitaniak T., *Phys. Rev. E*, **95** (2017) 010203.
[4] Bera B. K., Majhi S., Ghosh D. and Perc M., *EPL*, **118** (2017) 10001.
[5] Wojewoda J., Czolczynski K., Maistrenko Y. and Kapitaniak T., *Sci. Rep.*, **6** (2016) 34329.
[6] Wu Z.-M., Cheng H.-Y., Feng Y., Li H.-H., Dai Q.-L. and Yang J.-Z., *Front. Phys.*, **13** (2018) 130503.
[7] Rakshit S., Bera B. K., Perc M. and Ghosh D., *Sci. Rep.*, **7** (2017) 2412.
[8] Kuramoto Y. and Battogtokh D., *Nonlinear Phenom. Complex Syst.*, **5** (2002) 380.
[9] Rattenborg N. C., Amlaner C. J. and Lima S. L., *Neurosci. Biobehav. Rev.*, **24** (2000) 817.
[10] Andrzejak R. G., Rummel C., Mormann F. and Schindler K., *Sci. Rep.*, **6** (2016) 23000.
[11] Hizanidis J., Kouvaris N. E., Zamora-López G., Díaz-Guilera A. and Antonopoulos C. G., *Sci. Rep.*, **6** (2016) 19845.
[12] González-Avella J. C., Cosenza M. G. and San Miguel M., *Phys. A: Stat. Mech. Appl.*, **399** (2014) 24.
[13] Martens E. A., Laing C. R. and Strogatz S. H., *Phys. Rev. Lett.*, **104** (2010) 044101.
[14] Laing C. R., *Phys. Rev. E*, **92** (2015) 050904.
[15] Schmidt L., Schönleber K., Krischer K. and García-Morales V., *Chaos*, **24** (2014) 013102.
[16] Ulonska S., Omelchenko I., Zakharova A. and Schöll E., *Chaos*, **26** (2016) 094825.
[17] Dudkowski D., Maistrenko Y. and Kapitaniak T., *Chaos*, **26** (2016) 116306.
[18] Hagerstrom A. M., Murphy T. E., Roy R., Hövel P., Omelchenko I. and Schöll E., *Nat. Phys.*, **8** (2012) 658.
[19] Bera B. K., Ghosh D. and Lakshmanan M., *Phys. Rev. E*, **93** (2016) 012205.
[20] Hizanidis J., Kanas V. G., Bezerianos A. and Bountis T., *Int. J. Bifurcat. Chaos*, **24** (2014) 1450030.
[21] Majhi S., Perc M. and Ghosh D., *Sci. Rep.*, **6** (2016) 39033.
[22] Shepelev I. A., Vadivasova T. E., Bukh A., Strelkova G. and Anishchenko V., *Phys. Lett. A*, **381** (2017) 1398.
[23] Tinsley M. R., Nkomo S. and Showalter K., *Nat. Phys.*, **8** (2012) 662.
[24] Viktorov E. A., Habruseva T., Hegarty S. P., Huyet G. and Kelleher B., *Phys. Rev. Lett.*, **112** (2014) 224101.
[25] Martens E. A., Thutupalli S., Fourrière A. and Hallatschek O., *Proc. Natl. Acad. Sci. U.S.A.*, **110** (2013) 10563.
[26] Bogomolov S. A., Slepnev A. V., Strelkova G. I., Schöll E. and Anishchenko V. S., *Commun. Nonlinear Sci. Numer. Simul.*, **43** (2017) 25.
[27] Zakharova A., Kapeller M. and Schöll E., *Phys. Rev. Lett.*, **112** (2014) 154101.
[28] Majhi S., Muruganandam P., Ferreira F. F., Ghosh D. and Dana S. K., *Chaos*, **28** (2018) 081101.
[29] Abrams D. M., Mirollo R., Strogatz S. H. and Wiley D. A., *Phys. Rev. Lett.*, **101** (2008) 084103.
[30] Kapitaniak T., Kuzma P., Wojewoda J., Czolczynski K. and Maistrenko Y., *Sci. Rep.*, **4** (2014) 6379.
[31] Parastesh F., Jafari S., Azarnoush H., Hatef B. and Bountis A., *Chaos, Solitons Fractals*, **110** (2018) 203.
[32] Xie J., Knobloch E. and Kao H.-C., *Phys. Rev. E*, **90** (2014) 022919.
[33] Majhi S. and Ghosh D., *Chaos*, **28** (2018) 083113.
[34] Martens E. A., Laing C. R. and Strogatz S. H., *Phys. Rev. Lett.*, **104** (2010) 044101.
[35] Song X., Wang C., Ma J. and Tang J., *Sci. China Technol. Sci.*, **58** (2015) 1007.
[36] Lv M. and Ma J., *Neurocomputing*, **205** (2016) 375.
[37] Bao B., Hu A., Xu Q., Bao H., Wu H. and Chen M., *Nonlinear Dyn.*, **92** (2018) 1695.
[38] Majhi S., Perc M. and Ghosh D., *Chaos*, **27** (2017) 073109.
[39] Kundu S., Majhi S., Bera B. K., Ghosh D. and Lakshmanan M., *Phys. Rev. E*, **97** (2018) 022201.
[40] Sethia G. C., Sen A. and Johnston G. L., *Phys. Rev. E*, **88** (2013) 042917.
[41] Bera B. K., Ghosh D. and Banerjee T., *Phys. Rev. E*, **94** (2016) 012215.
[42] Bera B. K and Ghosh D., *Phys. Rev. E*, **93** (2016) 052223.